

Accepted Manuscript

New direct inhibitors of InhA with antimycobacterial activity based on a tetrahydropyran scaffold

Stane Pajk, Matej Živec, Roman Šink, Izidor Sosič, Margarete Neu, Chun-wa Chung, María Martínez-Hoyos, Esther Pérez-Herrán, Daniel Álvarez-Gómez, Emilio Álvarez-Ruiz, Alfonso Mendoza-Losana, Julia Castro-Pichel, David Barros, Lluís Ballell-Pages, Robert J. Young, Maire A. Convery, Lourdes Encinas, Stanislav Gobec



PII: S0223-5234(16)30078-2

DOI: [10.1016/j.ejmech.2016.02.008](https://doi.org/10.1016/j.ejmech.2016.02.008)

Reference: EJMECH 8359

To appear in: *European Journal of Medicinal Chemistry*

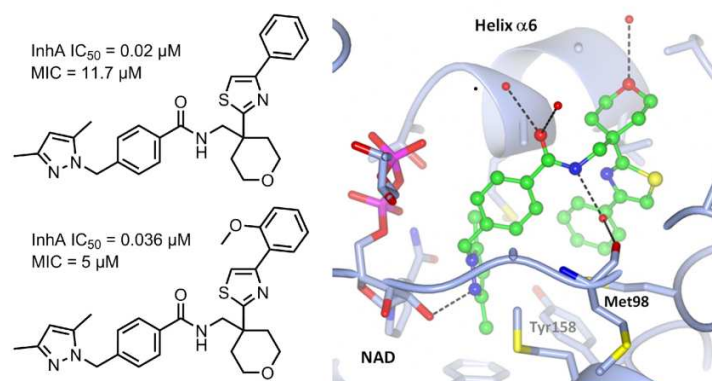
Received Date: 21 December 2015

Revised Date: 3 February 2016

Accepted Date: 4 February 2016

Please cite this article as: S. Pajk, M. Živec, R. Šink, I. Sosič, M. Neu, C.-w. Chung, M. Martínez-Hoyos, E. Pérez-Herrán, D. Álvarez-Gómez, E. Álvarez-Ruiz, A. Mendoza-Losana, J. Castro-Pichel, D. Barros, L. Ballell-Pages, R.J. Young, M.A. Convery, L. Encinas, S. Gobec, New direct inhibitors of InhA with antimycobacterial activity based on a tetrahydropyran scaffold, *European Journal of Medicinal Chemistry* (2016), doi: 10.1016/j.ejmech.2016.02.008.

This is a PDF file of an unedited manuscript that has been accepted for publication. As a service to our customers we are providing this early version of the manuscript. The manuscript will undergo copyediting, typesetting, and review of the resulting proof before it is published in its final form. Please note that during the production process errors may be discovered which could affect the content, and all legal disclaimers that apply to the journal pertain.



New direct inhibitors of InhA with antimycobacterial activity based on a tetrahydropyran scaffold

Stane Pajk,[†] Matej Živec,[†] Roman Šink,[†] Izidor Sosič,[†] Margarete Neu,[¶] Chun-wa Chung,[¶] María Martínez-Hoyos,[‡] Esther Pérez-Herrán,[‡] Daniel Álvarez-Gómez,[‡] Emilio Álvarez-Ruíz,[‡] Alfonso Mendoza-Losana,[‡] Julia Castro-Pichel,[‡] David Barros,[‡] Lluís Ballell-Pages,[‡] Robert J. Young,[¶] Maire A. Convery,[¶] Lourdes Encinas,^{‡*} Stanislav Gobec^{†*}

[†]University of Ljubljana, Faculty of Pharmacy, Ljubljana, Slovenia

[‡]DPU TB Diseases of the Developing World, GlaxoSmithKline, Tres Cantos, Madrid, Spain

[¶]Medicines Research Centre, GlaxoSmithKline, Stevenage, Hertfordshire, UK

Corresponding Author

*For S. G.: Tel, +386 1 47 69 585; E-mail, stanislav.gobec@ffa-uni-lj.si

*For L. E.: Tel; +346 3 85 10 876; E-mail, lourdes.p.encinas-prieto@gsk.com

Abstract

Tetrahydropyran derivative **1** was discovered in a high-throughput screening campaign to find new inhibitors of mycobacterial InhA. Following initial *in-vitro* profiling, a structure-activity relationship study was initiated and a focused library of analogs was synthesized and evaluated. This yielded compound **42** with improved antimycobacterial activity and low cytotoxicity. Additionally, the crystal

structure of InhA in complex with inhibitor **1** was resolved, to reveal the binding mode and provide hints for further optimization.

1. Introduction

Tuberculosis (TB) remains a major global health problem, with an estimated 9 million new cases and 1.5 million deaths per year [1]. Although progress has been made to reduce the global incidence of TB, the emergence and spread of drug resistance threatens to undermine these efforts. This includes both multi-drug resistant TB, which is resistant to isoniazid and rifampicin, and extensively drug-resistant TB, which is resistant to isoniazid, rifampicin, any fluoroquinolone, and an injectable drug (i.e., one of capraomycin, kanamycin, amikacin) [2–4].

The mycobacterial fatty-acid biosynthesis pathway II (FAS-II) represents a validated target for drug discovery, as fatty acids are essential for bacterial growth and can only be synthesized *de novo*. In addition, the bacterial FAS-II system is fundamentally distinct from that of mammals, thus providing the possibility to selectively target bacteria [5]. One of the enzymes involved in the FAS-II pathway in *Mycobacterium tuberculosis* (*Mtb*) is InhA, a NADH-dependent, enoyl-acyl carrier protein reductase. This is the target of isoniazid, a first-line drug for treatment of TB. Isoniazid is a pro-drug that is enzymatically activated by KatG, a mixed function catalase/ peroxidase; this transforms isoniazid into an unstable species that reacts with the NAD cofactor to form a covalent adduct, which subsequently inhibits InhA activity. Resistance to isoniazid is mainly the result of mutations in KatG that reduce its activation of isoniazid, and to a lesser extent, to mutations in the InhA active site. Therefore, compounds that directly target InhA and do not require activation by the mycobacterial catalase/ peroxidase KatG are promising candidates for treatment of infections caused by isoniazid-resistant strains [6–7]. As a follow-up of previous reports, we present here the synthesis, physicochemical characterization, biological profiling, and initial structure-activity relationships (SARs) of new tetrahydropyran derivatives of hit compound **1** (Figure 1) that was identified by GlaxoSmithKline in a high-throughput screening (HTS) campaign against InhA.

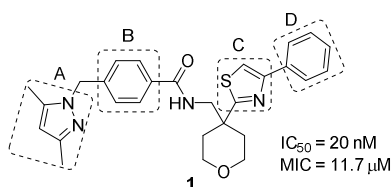


Figure 1. High-throughput screening hit compound **1**, with aromatic rings marked.

2. Results and discussion

2.1 Hit validation

Hit compound **1** was identified by high-throughput screening against InhA with the GlaxoSmithKline compound collection. First, compound **1** was re-synthesized (see below), to complete the initial round of *in-vitro* profiling, where it had good InhA inhibitory potency ($IC_{50} = 0.020 \mu M$), moderate *in-vitro* antimycobacterial activity (MIC = 11.7 μM), and killed *Mtb* inside macrophages (Table 1). In terms of early safety profiling, compound **1** showed modest hERG inhibition, with an IC_{50} of 50.1 μM , and low cytotoxicity against the HepG2 human cell line ($TOX_{50} = 100 \mu M$).

Table 1. Profile of compound **1**: *in-vitro* InhA inhibition, antitubercular activity, and physicochemical and preliminary safety properties.

MW	486.6	InhA IC_{50} (μM)	0.020
ClogP	4.18	<i>Mtb</i> MIC (μM)	11.7
Solubility CLND (μM)	115 ^a	Intracell IC_{90} (μM)	3.98
hERG IC_{50} (μM)	44.9	Cell tox HepG2 TOX_{50} (μM)	100

^a CLND, solubility values that are within 85% of maximum possible concentration (as determined from DMSO stock concentration).

We confirmed the relationship between InhA inhibition and antimycobacterial MIC through the use of an InhA_{MTB} overexpressor strain, which showed a 4-fold increase in MIC compared to the wild type (Table S1). Compound **1** was further evaluated against a panel of Gram-positive and Gram-negative

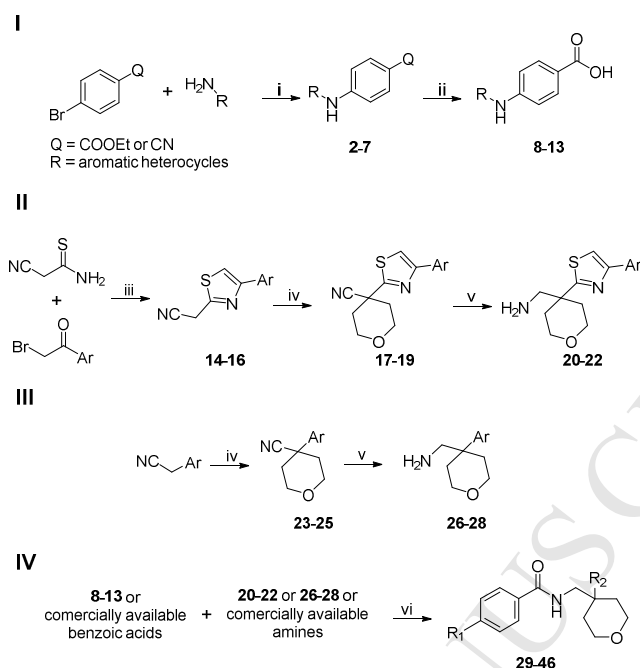
organisms, and it showed selective activity against *Mtb* H37Rv (Table S2). Additionally, it was tested against seven isoniazid-resistant clinical isolates with characterized mutations either in *katG* (high-level resistance to isoniazid) or in nucleotide position 15 upstream of the transcription start site for *inhA* (InhA over-expression) [8,9]. Mutations in codon 315 of *katG* and the *inhA* promoter are proven mechanisms of isoniazid resistance. Compound **1** showed a small upward shift in MIC against isoniazid resistance in general, but a more significant shift was observed in the group of strains that overexpressed InhA. An increased MIC of isoniazid was observed in paired clinical isolates with mutations in codon 315 of *katG* (Table S3). Analysis of the drug susceptibility of these isolates confirmed that strains carrying the *katG* mutation showed a high level of resistance to isoniazid (MIC >25 µg/ml) while susceptibility to compound **1** was similar to wild-type (MIC = 15.6-62.5 µM). A moderate shift in MIC was observed against the group of strains overexpressing InhA, for both compounds.

2.2 Synthesis and structure-activity relationships

A chemistry-driven approach was used to study the initial SARs of compound **1**. The goal of this approach was to explore the chemical space through the introduction of structural changes to rings A, C, and D, while leaving ring B and the *N*-((tetrahydro-2*H*-pyran-4-yl)methyl)amide core in place (Figure 1).

Compound **1** and related analogs **29-46** were synthesized according to the convergent route presented in Scheme 1. To explore the chemical space around ring A, we used either commercially available 4-substituted benzoic acids or derivatives **8-13**, which we synthesized (Scheme 1, IV).

The possibility of replacing the methylene linker between rings A and B with an amino group (Figure 1) was assessed. In the first step, palladium-catalyzed *N*-arylation between 4-bromobenzonitrile or 4-bromobenzoate and commercially available heteroaryl amines yielded the appropriate 4-substituted benzoic acid precursors **2-7** (Scheme 1, I) [10–12]. These were then hydrolyzed to the corresponding carboxylic acids **8-13**; acid-catalyzed hydrolysis [13] was used in the case of nitriles **2-5**, and base-catalyzed hydrolysis in the case of esters **6** and **7**.

Scheme 1. Synthesis of compounds **2-46**^a

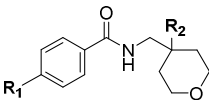
^aReagents and conditions: (i) Pd₂dba₃, BrettPhos, K₂CO₃, AcOH, molecular sieves 3 Å, *tert*-butanol, 115 °C, 3 h; (ii) HCl_(conc), 105 °C, 3 h (for Q = CN) or KOH, 50 °C, 15 h (for Q = COOEt); (iii) THF, Et₃N, rt, 2 h; (iv) (ClCH₂CH₂)₂O, DMF, NaH, 0 °C to rt, 4 h; (v) THF, LiAlH₄, 0 °C to rt, 4 h; (vi) TBTU, Et₃N, CH₂Cl₂, 0 °C to rt, 1 h, or HATU, Et₃N, DMF, 0 °C to rt, 1 h. For R₁ and R₂, see Table 2.

With the aim of exploring the substituent tolerance of ring D (Scheme 1, II), we prepared different amines as precursors **20-22**. Initially, 2-bromoacetophenone or its derivatives were reacted with 2-cyanothioacetate to form the thiazoles **14-16** [14]. In the next step, the tetrahydropyran ring was introduced (compounds **17-19**), followed by the reduction of the nitrile moiety with LiAlH₄, to give amines **20-22** [15].

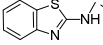
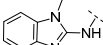
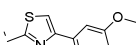
For the final set of modifications, ring D was omitted, and the thiazole of ring C was replaced by differently substituted phenyls or pyridin-2-yl. The synthetic strategy was the same as for the synthesis of amines **20-22**, except without the first step (Scheme 1, III). The tetrahydropyran ring was constructed by double alkylation of commercial 2-aryl acetone nitriles with dichlorodiethylether, to yield compounds **23-25**. This was followed by reduction of the nitrile moiety to give the desired amines **26-28**. Commercially available or synthesized amines and benzoic acid derivatives were finally coupled

to give the target compounds **29-46** (Scheme 1, IV; Table 2). The prepared compounds were then tested for InhA inhibition, antimycobacterial activity against *Mtb* H37Rv, and cytotoxicity in the HepG2 cell line (Table 2).

Table 2. Inhibitory potencies and antimycobacterial potencies of compounds **1** and **29-46** against *M. tuberculosis* InhA, and their clogP data, solubility, and cytotoxicity.



Cpd	R ₁	R ₂	InhA		clogP	CLND ^a (μM)	Cell tox HepG2 TOX ₅₀ (μM)
			IC ₅₀ (μM)	MIC (μM)			
1			0.02	11.7	4.18	115	100 (SI=8.5)
29			> 1	> 125	4.14	≥396	79.4
30			> 1	> 125	2.76	138	>100
31			>100	80	4.56	33	87.1
32			> 1	> 125	3.26	193	> 100
33			> 10	125	2.42	191	> 100
34			> 1	125	3.04	71	79.4
35			5.56	> 125	3.08	48	79.4
36			> 10	> 80	4.4	<1	> 100

37			> 10	> 125	5.5	4	12.6
38			> 10	> 80	4.04	12	63.1
39			> 10	> 125	3.2	29	63.1
40			> 10	94	4.95	10	20
41			0.323	20	4.2	72	50.1
42			0.036	5	3.64	78	50.1 (SI=10.0)
43			6.38	> 125	3.2	≥458	> 100
44			7.94	125	3.25	≥478	> 100
45			> 10	> 125	1.78	≥445	> 100
46			0.029	16	5.17	77	79.4 (SI=5.0)

^a CLND, solubility values that are within 85% of maximum possible concentration (as determined from DMSO stock concentration).

Correlation was found between InhA inhibition in the biochemical assay and antimycobacterial activity for compounds with IC₅₀ values lower than 1 μM. Above this threshold, the poor aqueous solubility of some of the compounds was most likely the factor responsible for the lower levels of correlation. We defined the ratio between the TOX₅₀ in HepG2 cells and the *Mtb* H37Rv MIC as the selectivity index (SI). Among the compounds active against *Mtb* H37Rv, only compound **42** showed a SI >10 and could be considered noncytotoxic (Table 2). From the data in Table 2, it appears that

achieving nanomolar InhA inhibitory potency not only results in good antimycobacterial potency, but also leads to less off-target binding, and consequently to lower cytotoxicity.

Compounds **29-34** were synthesized to determine the importance of the 3,5-dimethyl pyrazole moiety (ring A) and the consequent decrease in lipophilicity. Compound **1** had a relatively high clogP of 4.18 [16]. The introduction of aliphatic heterocycles in place of ring A (compounds **29, 30**) resulted in loss of InhA inhibitory potency along with the antimycobacterial activity, regardless of the presence of the methylene linker between rings A and B. Furthermore, the absence of the methylene linker between rings A and B (compounds **31-34**) resulted in complete loss of antimycobacterial activity regardless of the aromatic heterocycle in the place of ring A. We hypothesized that replacement of the methylene linker between rings A and B with the amino group might contribute towards the formation of additional hydrogen bonds in the InhA active site, while at the same time simplifying the synthetic introduction of different aromatic heterocycles. However, this substitution yielded compounds **35-40** with IC_{50} values $>10 \mu M$.

Finally, the impact of substitutions in the phenyl ring (ring D) and the importance of the thiazole group (ring C) were explored (compounds **41-46**). Introduction of the methoxy group to the *meta*-position of ring D was allowed, as compound **41** showed moderate inhibition of InhA, with an IC_{50} of $0.323 \mu M$. The introduction of the methoxy to the *ortho*-position of ring D resulted in InhA inhibitory potency in the nanomolar range (compound **42**, $IC_{50} = 40 \text{ nM}$) and antimycobacterial potency comparable to the initial hit compound **1**. These data suggest that substitution of the phenyl ring is a suitable space for further optimization in the future. Reductions in the number of heterocycles, omission of ring D, and introduction of differently substituted phenyl moieties (compounds **43, 44**) or pyridin-2-yl (compound **45**) in place of ring C resulted in substantial loss of the enzymatic and whole cell inhibition potencies. The replacement of the thiazole ring (ring C) of compound **1** with a phenyl ring (compound **46**) led to a compound with good InhA inhibition and antimycobacterial potency, despite poor aqueous solubility.

2.3 Crystal structure

To understand the nature of the specific interactions that underpin InhA inhibition by these tetrahydropyran derivatives, we solved the X-ray crystal structure of compound **1** bound to InhA in the presence of the cofactor, NAD (see Figure 2). The crystal structure shows that compound **1** adopts a U-shape and binds to InhA in the cleft that is normally occupied by substrate (Figure S2a). The overall binding position of compound **1** is similar to that observed for the pyrrolidine compound in the crystal structure (pdb entry 4COD, Figure S2b) [17]. The pyrazole on the left-hand side of compound **1** stacks against the pyridine portion of the NAD, and the pyrazole 2-nitrogen provides a H-bond interaction with the 2'-hydroxyl group of NAD. The InhA substrate-binding loop, which includes helix α_6 , is ordered in the structure, and the N-terminal end forms part of the pyrazole binding pocket. The methylene linker on the left-hand side of the molecule introduces a kink into the ligand that is necessary to maintain its shape complementarity with the binding site. The central amide of compound **1** has water-bridged interactions with the protein, including the backbone carbonyl of Met98. The tetrahydropyran points out of the binding site. The right-hand side of the molecule is in a deep pocket in the protein that is bound on one side by the C-terminal end of ordered helix α_6 ; it does not have any specific interactions with the protein.

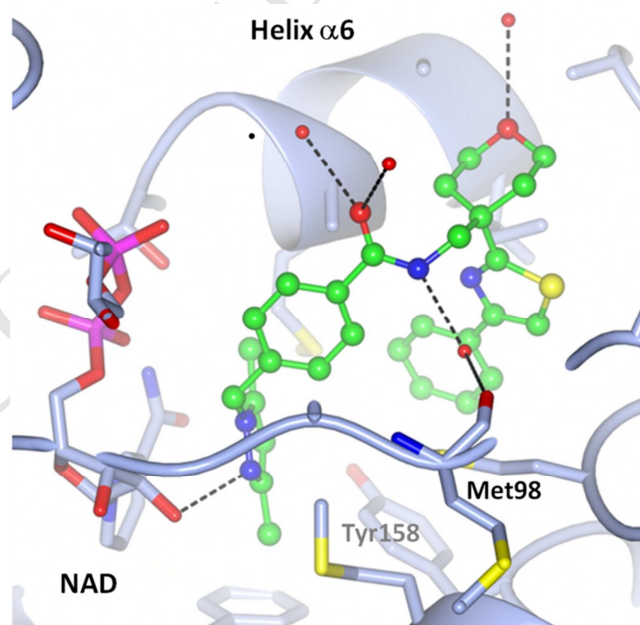


Figure 2. Compound **1** bound to the active site of InhA. Compound **1** is shown in green ball-and-sticks, NAD in thick gray lines, and hydrogen bonds in dashed lines. Helix α_6 is ordered in the structure, with Met98 and Tyr158 highlighted. Tyr158 adopts an apo orientation.

3. Conclusions

The tetrahydropyran compound **1** was identified in a high-throughput screen of the GlaxoSmithKline collection, and it showed good InhA inhibitory potency ($IC_{50} = 0.020 \mu M$), moderate *in-vitro* antimycobacterial activity ($MIC = 11.7 \mu M$), modest hERG inhibition, and low cytotoxicity against the HepG2 human cell line. Following initial *in-vitro* profiling, a SAR study was initiated and a series of 18 analogs was synthesized and evaluated. Based on the SAR data generated, it appears that rings C and D can be modified in further optimization efforts. The best compound **42** in this series demonstrated InhA inhibitory potency in the nanomolar range ($IC_{50} = 40 \text{ nM}$), antimycobacterial potency comparable to compound **1** ($MIC = 5 \mu M$), and a reasonable SI. Additionally, the crystal structure of compound **1** bound into InhA provided information on the binding mode, rationalised the SARs, and provided insight into the opportunities for further structure-based optimisation of InhA inhibitors.

4. Experimental section

4.1 Materials and methods. Chemicals from Sigma-Aldrich, TCI, and Acros were used without further purification. All reactions were performed under argon atmosphere, unless otherwise stated. Analytical TLC was performed on Merck silica gel (60 F₂₅₄) plates (0.25 mm) and visualized with ultraviolet light. Melting points were determined on a Reichert hot-stage microscope and are uncorrected. ¹H and ¹³C NMR spectra were recorded on a Bruker AVANCE III 400 MHz NMR spectrometer in CDCl₃ and DMSO-*d*₆ solution, with TMS or residual non-deuterated solvent as the internal standards. Mass spectra were recorded using a VG-Analytical Q-TOF Premier mass spectrometer.

4.2 General procedures

4.2.1 General procedure for the palladium-catalyzed *N*-arylation (compounds 2-7). An oven-dried pressure tube equipped with a magnetic stirring bar was charged with Pd₂dba₃ (4.7 mg, 0.51 mol %), BrettPhos (11.3 mg, 2.1 mol %), K₂CO₃ (192 mg, 1.4 mmol, 1.4 equiv.), aryl amine (1 mmol, 1 equiv.), aryl bromide (1 mmol, 1 equiv.), and activated molecular sieves of 4 Å (100 mg). The vessel was flushed well with argon. Dry *tert*-butanol (4 mL) and acetic acid (1.7 μL, 3 mol %) were added, and the pressure tube was sealed with a Teflon screw cap and placed into an oil bath at 115 °C for 3 h. The reaction mixture was then cooled to room temperature and filtered. The solvent was removed under reduced pressure, and the crude product was purified by flash chromatography. In the case where the aryl bromide (ethyl 4-bromobenzoate) was a liquid, it was added after *tert*-butanol.

4.2.2 General procedure for the hydrolysis of nitriles to carboxylic acids (compounds 8-11). The pressure tube equipped with a magnetic stirring bar was charged with nitrile and concentrated aqueous HCl (up to two thirds of the volume). The pressure tube was sealed with a Teflon screw cap and placed into an oil bath at 105 °C for 15 h. The reaction mixture was cooled to room temperature and the solvent removed under reduced pressure, to yield the crude product.

4.2.3 General procedure for the hydrolysis of esters to carboxylic acids (compounds 12, 13). The ester (0.3 mmol) was dissolved in a mixture of dioxane (4 mL) and water (3 mL). Powdered KOH (168 mg, 3.0 mmol, 10 equiv.) was added to this solution, and the reaction mixture was stirred at 50 °C overnight.

4.2.4 General procedure for the Hantzsch thiazole synthesis (compounds 14-16). The corresponding 2-bromo-1-(aryl)ethan-1-one derivative (0.02 mol, 1 equiv.) and 2-cyanothioacetamide (0.02 mol, 1 equiv.) were dissolved in dry THF (50 mL) followed by the addition of Et₃N (0.022 mol, 1.1 equiv.) (precipitation of a white solid). The reaction mixture was left to react at room temperature overnight. The solid was filtered off and the filtrate was concentrated on a rotary evaporator. The residue was dissolved in EtOAc (200 mL) and washed with water (2× 50 mL), saturated aqueous solution of NaHCO₃ (2× 50 mL), and brine (50 mL), and dried over Na₂SO₄. The solvent was evaporated under reduced pressure.

4.2.5 General procedure for the formation of the tetrahydropyran ring (compounds 17-19, 23-25). The corresponding arylacetonitrile derivative (15.6 mmol, 1 equiv.) and bis(chloroethyl) ether (15.6 mmol, 1 equiv.) were dissolved in dry DMF (50 mL), and cooled in an ice-bath. Argon was passed through the solution, followed by addition of 60% suspension of NaH in mineral oil (31.2 mmol, 2 equiv.), in small portions over 20 min. Then, the ice-bath was removed and the reaction mixture was heated at 55 °C for 5 h, with the reaction then quenched with water. The reaction mixture was diluted with EtOAc (300 mL), washed with 1 M aqueous HCl (3× 70 mL) and brine (2× 50 mL), and dried over Na₂SO₄. The solvent was evaporated under reduced pressure.

4.2.6 General procedure for the reduction of nitriles to amines (compounds 20-22 and 26-28). A solution of a corresponding nitrile derivative (1.00 mmol, 1 equiv.) in freshly distilled THF (5 mL) was cooled in an ice-bath, and LiAlH₄ (1.25 mmol, 1.25 equiv.) was added. The reaction mixture was allowed to react overnight at room temperature, cooled in an ice-bath, and quenched with saturated aqueous solution of NaHCO₃ (20 mL). The aqueous phase was extracted with EtOAc (3× 30 mL), the combined organic fractions were dried over Na₂SO₄, and the solvent was evaporated under reduced pressure.

4.2.7 General procedure for the coupling of amines and carboxylic acids A (compounds 1, 29-34, 41-46). To a solution of benzoic acid derivative (0.50 mmol, 1 equiv.) in CH₂Cl₂ (7.5 mL) cooled in an ice-bath, Et₃N (1.50 mmol, 3 equiv.) and TBTU (0.65 mmol, 1.3 equiv.) were added. After 10 min, the corresponding amine (0.50 mmol, 1 equiv.) was added, and the reaction mixture was left to react for 1 h at room temperature. The reaction mixture was diluted with CH₂Cl₂ (30 mL) and the organic phase was washed with 1 M aqueous HCl (3× 15 mL), saturated aqueous solution of NaHCO₃ (3× 15 mL), and brine (30 mL), and dried over Na₂SO₄. The solvent was evaporated under reduced pressure.

4.2.7.1 4-((3,5-dimethyl-1H-pyrazol-1-yl)methyl)-N-((4-(4-phenylthiazol-2-yl)tetrahydro-2H-pyran-4-yl)methyl)benzamide (1). Compound **1** was prepared as described under the general procedure for the coupling of amines and carboxylic acids (coupling A). The crude product was purified by flash chromatography on silica gel (DCM:MeOH = 1:0 to 10:1), to give the desired

product (71%) as a white solid. ^1H NMR (400 MHz, CDCl_3): δ (ppm) 1.90-2.05 (m, 2H), 2.13 (s, 3H), 2.20-2.40 (m, 2H), 2.28 (s, 3H), 3.65-3.80 (m, 2H), 3.82 (d, $J = 0.3$ Hz, 2H), 3.85-4.00 (m, 2H), 5.27 (s, 2H), 5.89 (s, 1H), 7.00-7.15 (m, 2H), 7.30-7.45 (m, 4H), 7.50 (s, 1H), 7.65-7.80 (m, 2H), 7.85-7.95 (m, 2H). MS (ESI) m/z $[\text{M}+\text{H}]^+ = 487.0$.

4.2.7.2 4-((3,5-Dimethyl-1H-pyrazol-1-yl)methyl)-N-((4-(4-(2-methoxyphenyl)thiazol-2-yl)tetrahydro-2H-pyran-4-yl)methyl)benzamide (42). Compound **42** was prepared as described under the general coupling A procedure. The product was purified by flash chromatography (CH_2Cl_2 :MeOH, 30:1), to give the desired product (49%) as yellow crystals. ^1H NMR (400 MHz, $\text{DMSO}-d_6$): δ (ppm) 1.80-2.00 (m, 2H), 2.10 (s, 3H), 2.13 (s, 3H), 2.15-2.3 (m, 2H), 3.30-3.35 (m, 2H), 3.51 (d, 2H, $J = 5.6$ Hz), 3.70-3.90 (m, 2H), 3.91 (s, 3H), 5.22 (s, 2H), 5.86 (s, 1H), 6.92-7.00 (m, 1H), 7.02-7.14 (m, 2H), 7.28-7.38 (m, 1H), 7.68-7.74 (m, 2H), 8.04 (s, 1H), 8.10-8.18 (m, 1H), 8.40 (t, 1H, $J = 5.6$ Hz). ^{13}C NMR (100 MHz, $\text{DMSO}-d_6$): δ (ppm) 10.63, 13.36, 14.11, 20.78, 34.18, 38.26, 43.94, 49.34, 51.19, 54.93, 55.47, 59.77, 63.58, 105.09, 111.62, 117.76, 120.40, 122.63, 126.56, 127.61, 128.90, 129.48, 133.64, 138.84, 141.10, 146.22, 149.57, 156.39, 166.53, 172.16. HRMS (ESI), m/z calcd for $\text{C}_{29}\text{H}_{33}\text{N}_4\text{O}_3\text{S}$ 517.2273 ($\text{M}+\text{H}$) $^+$, found 517.2266.

4.2.8 General procedure for the coupling of amines and carboxylic acids B (compounds 35-40).

The corresponding carboxylic acid (0.20 mmol, 1 equiv.), Et_3N (82 μL , 0.59 mmol, 3 equiv.) and compound **6** (54 mL, 0.20 mmol, 1 equiv.) were dissolved in DMF (4 mL) and cooled in an ice bath. HATU (106.5 mg, 0.28 mmol, 1.4 equiv.) was added to the reaction mixture, the temperature of the reaction mixture was then allowed to reach room temperature, and the stirring was continued for 4 h. The solvent was evaporated under reduced pressure and the residue was dissolved in EtOAc (30 mL). The organic phase was washed with 0.1 M aqueous HCl (10 mL), saturated aqueous solution of NaHCO_3 (10 mL), and saturated aqueous solution of NH_4Cl (2×10 mL), and dried over Na_2SO_4 . The solvent was evaporated under reduced pressure.

Appendix A. Supplementary data

Additional Tables, Schemes, Figures, protocols and experimental procedures of some of the assays mentioned in the main text are available at xxx.

Funding Sources

The research leading to these data has received funding from the Global Alliance for TB Drug Development, and from the European Union 7th Framework Program (FP7- 2007-2013) under Orchid Grant agreement No. 261378. The funders had no role in the study design, data collection and analysis, decision to publish, or preparation of the manuscript.

Acknowledgment

We thank Dr. Chris Berrie for critical reading of the manuscript. We are grateful to Rubén González del Río, Delia Blanco Ruano, Pedro A. Torres Gómez, Lydia Mata, Francisco de Dios, and Vanessa Barroso for the biological evaluation, and Bill McDowell for preparation of the protein.

References

1. WHO Global Tuberculosis Report 2014; World Health Organization: Geneva, 2014. Available: http://www.who.int/tb/publications/global_report/en/ (accessed: February 28, 2015).
2. N. R. Gandhi, P. Nunn, K. Dheda, H. S. Schaaf, M. Zignol, D. van Soolingen, P. Jensen, J. Bayona, Multidrug-resistant and extensively drug-resistant tuberculosis: A threat to global control of tuberculosis, *Lancet* 375 (2010) 1830-1843.
3. N. S. Shah, W. Abigail, B. Gill-Han, B. Lucia, B. Fadila, M.-C. Nuria, D. Francis, G. Chris, H. Marta, L. Rosario, L. Richard, M. Beverly, P. Françoise, R. Maria Filomena, R.-G. Sabine, D. Armand Van, V. Veronique, F. L. Kayla, W. Charles, J. P. Cegielski, Worldwide emergence of extensively drug-resistant tuberculosis, *Emerg. Infect. Dis.* 13 (2007) 380.
4. Z. Ma, C. Lienhardt, H. McIlleron, A. J. Nunn, X. Wang, Global tuberculosis drug development pipeline: the need and the reality, *Lancet* 375 (2010) 2100-2109.

5. H. Lu, P. J. Tonge, Inhibitors of FabI, an enzyme drug target in the bacterial fatty acid biosynthesis pathway, *Accounts Chem. Res.* 41 (2008) 11-20.
6. P.E. Almeida Da Silva, J. C. Palomino, Molecular basis and mechanisms of drug resistance in *Mycobacterium tuberculosis*: classical and new drugs, *J. Antimicrob. Chemoth.* 66 (2011) 1417-1430.
7. M. R. Kuo, H. R. Morbidoni, D. Alland, S. F. Sneddon, B. B. Gourlie, M. M. Staveski, M. Leonard, J. S. Gregory, A. D. Janjigian, C. Yee, J. M. Musser, B. Kreiswirth, H. Iwamoto, R. Perozzo, W. R. Jacobs, J. C. Sacchettini, D. A. Fidock, Targeting tuberculosis and malaria through inhibition of enoyl reductase: compound activity and structural data. *J. Biol. Chem.* 278 (2003) 20851-20859.
8. C. Vilchèze, R. William, J. Jacobs, The mechanism of isoniazid killing: clarity through the scope of genetics, *Annu. Rev. of Microbiol.* 61 (2007) 35-50.
9. A. Sandgren, M. Strong, P. Muthukrishnan, B. K. Weiner, G. M. Church, M. B. Murray, Tuberculosis drug resistance mutation database, *PLoS Med.* 6 (2009) e1000002.
10. D. Maiti, B. P. Fors, J. L. Henderson, Y. Nakamura, S. L. Buchwald, Palladium-catalyzed coupling of functionalized primary and secondary amines with aryl and heteroaryl halides: two ligands suffice in most cases, *Chem. Sci.* 2 (2011) 57-68.
11. M. A. McGowan, J. L. Henderson, S. L. Buchwald, Palladium-catalyzed N-Arylation of 2-aminothiazoles, *Org. Lett.* 14 (2012) 1432-1435.
12. D. S. Surry, S. L. Buchwald, Diamine ligands in copper-catalyzed reactions, *Chem. Sci.* 1 (2010) 13-31.
13. S. F. Wnuk, S. M. Chowdhury, P. I. Garcia, M. J. Robins, stereodefined synthesis of o3'-labeled uracil nucleosides. 3'-[17O]-2'-azido-2'-deoxyuridine 5'-diphosphate as a probe for the mechanism of inactivation of ribonucleotide reductases, *J. Org. Chem.* 67 (2002) 1816-1819.
14. J. Mulzer, A. Mantoulidis, E. Öhler, Total syntheses of epothilones B and D, *J. Org. Chem.* 65 (2000) 7456-7467.

15. E. Baloglu, S. Ghosh, M. Lobera, D. Schmidt, Compounds and methods. US 2012/0322827 A1, December 20, 2012.
16. M. Hann, Molecular Obesity, potency and other addictions in drug discovery, in: G. Scapin, D. Patel, E. Arnold (Eds.), Multifaceted roles of crystallography in modern drug discovery, Springer, Netherlands, 2015, pp. 183-196.
17. R. Šink, I. Sosič, M. Živec, R. Fernandez-Menendez, S. Turk, S. Pajk, D. Alvarez-Gomez, E. M. Lopez-Roman, C. Gonzales-Cortez, J. Rullas-Triconado, I. Angulo-Barturen, D. Barros, L. Ballell-Pages, R. J. Young, L. Encinas, S. Gobec, Design, synthesis, and evaluation of new thiadiazole-based direct inhibitors of enoyl acyl carrier protein reductase (InhA) for the treatment of tuberculosis, *J. Med. Chem.* 58 (2014) 613-624.

Highlights

- New tetrahydropyran inhibitor (**1**) of mycobacterial InhA was discovered.
- It exhibits good InhA inhibitory potency and moderate antimycobacterial activity.
- SAR study was initiated and a focused library of analogs of hit **1** was synthesized.
- Crystal structure of inhibitor **1** bound to InhA revealed the binding mode.